

## RESEARCH ARTICLE

# Parasite-derived microRNA let-7-5p detection for metacestodiasis based on rolling circular amplification-assisted CRISPR/Cas9

Liqun Wang<sup>1</sup>  | Guiting Pu<sup>1</sup>  | Tingli Liu<sup>1</sup>  | Guoliang Chen<sup>1</sup>  | Hong Li<sup>1</sup>  |  
Tharheer Oluwashola Amuda<sup>1</sup>  | Shanling Cao<sup>1</sup>  | Hongbin Yan<sup>1</sup>  |  
Hong Yin<sup>1,2</sup>  | Baoquan Fu<sup>1,2</sup>  | Xuenong Luo<sup>1,2</sup> 

<sup>1</sup>State Key Laboratory for Animal Disease Control and Prevention, Key Laboratory of Veterinary Parasitology of Gansu Province, National Para-reference Laboratory for Animal Echinococcosis, Lanzhou Veterinary Research Institute, Chinese Academy of Agricultural Sciences (CAAS), Lanzhou, China

<sup>2</sup>Jiangsu Co-Innovation Center for the Prevention and Control of Important Animal Infectious Disease and Zoonoses, Yangzhou University, Yangzhou, China

**Correspondence**

Baoquan Fu and Xuenong Luo, State Key Laboratory of Veterinary Etiological Biology, Lanzhou Veterinary Research Institute, Chinese Academy of Agricultural Sciences, 1 Xujiaping, Yanchangbu, Lanzhou 730046, Gansu, The People's Republic of China. Email: [fubaoquan@caas.cn](mailto:fubaoquan@caas.cn) and [luoxuenong@caas.cn](mailto:luoxuenong@caas.cn)

**Funding information**

MOST | National Natural Science Foundation of China (NSFC), Grant/Award Number: 32072889; MOST | National Key Research and Development Program of China (NKPs), Grant/Award Number: 2023YFD1802401

**Abstract**

Metacestodiasis is an infectious disease caused by the larval stage of cestode parasites. This disease poses a serious health hazard to wildlife, livestock, and humans, and it incurs substantial economic losses by impacting the safety of the livestock industry, the quality of meat production, and public health security. Unfortunately, there is currently no available molecular diagnostic method capable of distinguishing cysticercus- and *Echinococcus*-derived microRNAs (miRNAs) from other helminthes and hosts in the plasma of metacestode-infected animals. This study aims to develop a specific, sensitive, and cost-efficient molecular diagnostic method for cysticercosis and echinococcosis, particularly for early detection. The study developed a rolling circular amplification (RCA)-assisted CRISPR/Cas9 detection method based on parasite-derived miRNA let-7-5p. Using a series of dilutions of the let-7 standard, the limit of detection (LOD) of the qPCR, RCA, and RCA-assisted CRISPR/Cas9 methods was compared. The specificity of qPCR and CRISPR/Cas9 was evaluated using four artificially synthesized let-7 standards from different species. A total of 151 plasma samples were used to evaluate the diagnostic performance. Additionally, the study also assessed the correlation between plasma levels of let-7-5p, the number of *Taenia pisiformis* cysticerci, and the weight of *Echinococcus multilocularis* cysts. The results demonstrated that the RCA-assisted CRISPR/Cas9 assay could significantly distinguish let-7 from cestodes and other species, achieving a LOD of 10 aM; the diagnostic sensitivity and specificity for rabbit cysticercosis and mouse *E. multilocularis* were 100% and 97.67%, and 100% and 100%, respectively. Notably,

**Abbreviations:** AE, Alveolar echinococcosis; CBS, carbonate buffer solution; CE, Cystic Echinococcosis; dpi, days post infection; *E. multilocularis*, *Echinococcus multilocularis*; ELISA, Enzyme Linked Immunosorbent Assay; ESP, excretory/secretory product; FI, fluorescence intensity; HRP, horseradish peroxidase; LOD, limit of detection; miRNA, microRNA; OD, optical density; PP, padlock probe; PBS, phosphate buffered saline; RCA, rolling circular amplification; ROC, receiver operating characteristic; RT-qPCR, reverse transcription quantitative polymerase chain reaction; SPF, specific-pathogen-free; *T. pisiformis*, *Taenia pisiformis*; TP, Taqman probe; TMB, Tetramethylbenzidine.

This is an open access article under the terms of the [Creative Commons Attribution](https://creativecommons.org/licenses/by/4.0/) License, which permits use, distribution and reproduction in any medium, provided the original work is properly cited.

© 2024 The Author(s). *The FASEB Journal* published by Wiley Periodicals LLC on behalf of Federation of American Societies for Experimental Biology.

let-7-5p gradually increased in the plasma of *T. pisiformis*-infected rabbits from 15 days post infection (dpi), peaked at 60 dpi, and persisted until 120 dpi. In *E. multilocularis*-infected mice, let-7-5p gradually increased from 15 dpi and persisted until 90 dpi. Furthermore, the expression of let-7-5p positively correlated with the number of cysticerci and cyst weight. These results indicated that the let-7-5p-based RCA-assisted CRISPR/Cas9 assay is a sensitive and specific detection method that can be used as a universal diagnostic method for metacestodiasis, particularly for early diagnosis (15 dpi).

#### KEYWORDS

diagnosis, let-7-5p, metacestodiasis, plasma, RCA-assisted CRISPR/Cas9

## 1 | INTRODUCTION

The Cestodes of the Taeniidae family encompass a wide variety of species, posing a significant threat to the healthy development of animal husbandry and public health safety. Metacestodiasis, caused by *Taenia* spp. (such as *Taenia solium*, *Taenia pisiformis*, and others) and *Echinococcus* spp. (primarily *Echinococcus multilocularis* and *Echinococcus granulosus*), not only results in substantial human morbidity and mortality on a global scale, but also infects livestock, leading to immense economic losses.<sup>1</sup> *T. pisiformis* is highly prevalent in China, with infection rates of 20%–100% and mortality rates of 4%–23.69% in rabbits.<sup>2</sup> Additionally, this disease can lead to serious liver injury, ascites, weight loss, and reduced fecundity in infected animals.<sup>3,4</sup> Alveolar echinococcosis (AE), caused by *E. multilocularis*, primarily affects the liver of both humans and animals, resulting in conditions such as fibrosis, cirrhosis, cancer, and even death.<sup>5,6</sup> Therefore, early diagnosis of metacestodiasis plays a pivotal role in controlling disease progression and ensuring the health of humans and animals.

Currently, the diagnosis of metacestodiasis largely relies on serological and imaging examinations.<sup>7,8</sup> Serological diagnostic technologies, like the ELISA assay, have been reported to detect metacestodiasis, yet the challenge of a high false-positive rate remains a major concern.<sup>9</sup> Molecular diagnosis technologies, such as multiplex PCR, exhibit high sensitivity and specificity; however, their application is limited to the differential diagnosis of taeniasis in dogs and humans.<sup>8</sup> Hence, there is an urgent need to develop specific, sensitive, and cost-efficient molecular diagnostic methods for metacestodiasis.

MicroRNAs (miRNAs) are small (18–24 nt) endogenous non-coding RNA molecules that regulate the expression of their target genes, playing pivotal roles in various biological processes, including cell proliferation, differentiation, apoptosis, and stress response.<sup>10,11</sup> These miRNAs

can circulate and remain stable in biological fluids such as plasma/serum, urine, and feces.<sup>12,13</sup> Circulating miRNAs have been shown to resist RNase-induced degradation, changes in pH and temperature, and multiple freeze-thaw cycles, rendering them highly suitable as potential biomarkers in biological fluids.<sup>13</sup>

Recent studies have shown that parasite-derived miRNAs can be detected in the plasma/serum of parasite-infected hosts, indicating their potential as biomarkers for diagnosing parasite infections.<sup>14,15</sup> Parasite-derived miRNAs, such as miR-277 and miR-3479-3p, demonstrate promise as novel diagnostic biomarkers for detecting human *Schistosoma japonicum* infection.<sup>16</sup> Additionally, research has identified egr-miR-2a-3p as a potential diagnostic biomarker for cystic echinococcosis (CE).<sup>17</sup> Previous studies have revealed that cestodes share the same miRNA let-7 (let-7-5p),<sup>18</sup> which has been shown to be one of the highly expressed miRNAs in cestodes.<sup>19–21</sup> In addition, the expression level of let-7-5p was significantly upregulated in the serum and liver of metacestodes-infected animals and humans,<sup>22–24</sup> suggesting its potential as a target molecule for diagnosing metacestodiasis.

Due to the special characteristics of miRNAs, such as their small size, low content, and high sequence similarity, the direct and effective detection of miRNAs in plasma/serum remains a challenge. Currently, several common miRNA detection methods, including reverse transcription quantitative polymerase chain reaction (RT-qPCR),<sup>25,26</sup> northern blotting,<sup>27,28</sup> and microarray,<sup>29</sup> have been utilized for analyzing clinical samples. Although these methods have been widely considered as the most common and gold standard for miRNA analysis, they still have some shortcomings. For instance, qPCR is time-consuming and requires multiple steps, including primer design, miRNA extraction, reverse transcription, and qPCR itself.<sup>30,31</sup> Moreover, qPCR cannot discriminate against highly homologous miRNAs.<sup>32</sup> Other methods, such as northern blotting and microarray assays, suffer

from poor detection specificity and sensitivity, lengthy processes, and high detection costs.<sup>33,34</sup> These drawbacks limit their further applications.

Recently, isothermal amplification techniques have found widespread use for amplifying DNA and RNA.<sup>35-37</sup> The RCA technique, in particular, has been extensively employed in detecting miRNAs due to its simplicity, specificity, and high sensitivity. These methods could elongate short RNAs into long DNA products, offering potential avenues for amplifying miRNA input signals.<sup>38</sup>

Furthermore, CRISPR-Cas systems have shown great potential as diagnostic tools due to their unique sequence recognition properties and capability for nucleic acid cleavage.<sup>39</sup> Recent studies have pioneered multiple nucleotide detection techniques based on these methods.<sup>40</sup> A specific miRNA detection method was developed by integrating RCA and CRISPR/Cas9 for lung cancer and obtained a low fM level of sensitivity.<sup>41</sup> Additionally, an accurate and sensitive miRNA detection technology was established by combining garland RCA and CRISPR/Cas9-assisted signal generation.<sup>40</sup> Hence, the prospect of detecting parasite-derived miRNAs based on RCA and CRISPR/Cas9 appears feasible.

In this work, using larval cestode-derived miRNA let-7-5p as a target, we developed a specific, rapid, isothermal miRNA detection approach termed RCA-assisted CRISPR/Cas9 based on let-7-5p (Figure 1). We demonstrated that the RCA-assisted CRISPR/Cas9 assay based on let-7-5p enabled the detection of miRNA at a limit

as low as 10 aM and effectively differentiated cestode-derived let-7-5p from other helminthes. Moreover, this method exhibited excellent diagnostic performance when applied to 151 clinical samples. Thus, this method could serve as valuable technical support for the early diagnosis of metacestodiasis.

## 2 | MATERIALS AND METHODS

### 2.1 | Ethics statement

All animal experiments were approved by the Animal Ethics Committee of Lanzhou Veterinary Research Institute, Chinese Academy of Agricultural Sciences (Permit No. LVRIAEC2021-028) and were performed in strict accordance with the Good Animal Practice of Animal Ethics Procedures and Guidelines of the People's Republic of China.

### 2.2 | Materials

The sequence of primers, padlock probe (PP), Taqman probe (TP), and sgRNA were listed in Table S1 and were synthesized by Sangon Biotech (Shanghai, China). The let-7 standards from different species were synthesized by Guangzhou RiboBio Co., Ltd. (Guangzhou, China). Cas9 nuclease was purchased from Vazyme (Nanjing, China).

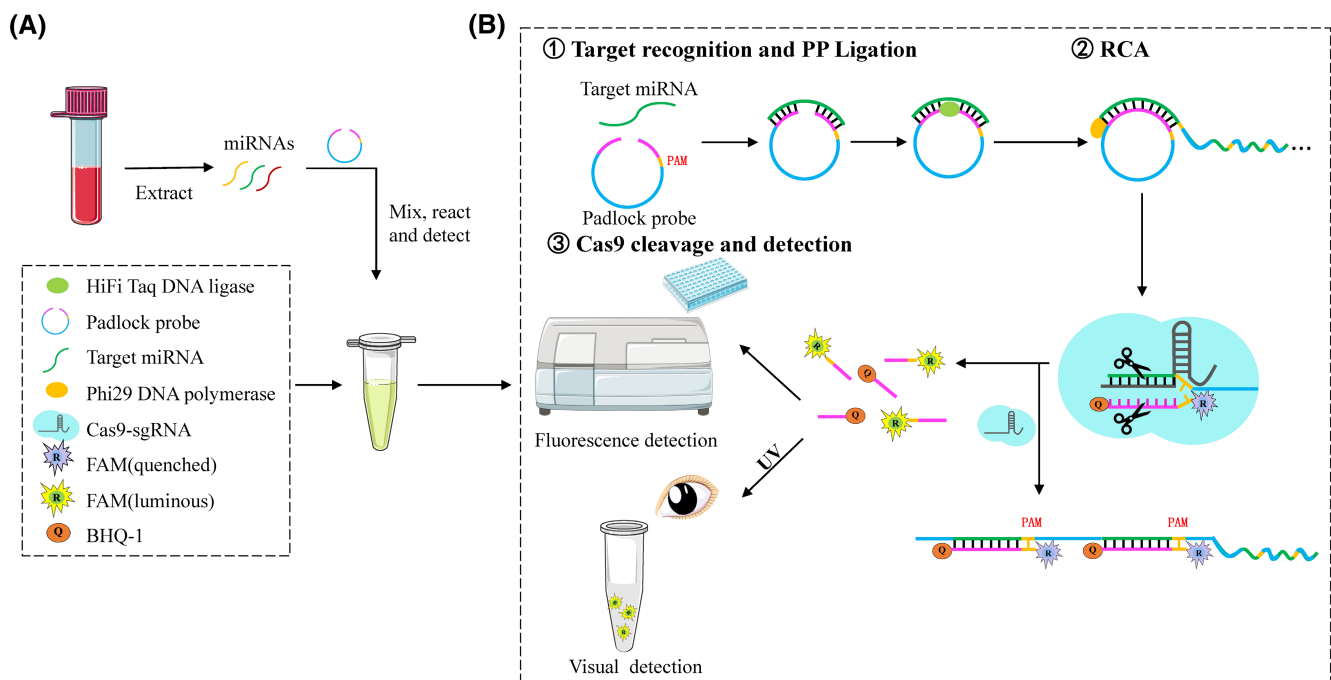


**FIGURE 1** The principle of RCA-assisted CRISPR/Cas9. (A) miRNA extraction and Rolling circular amplification (RCA)-CRISPR/Cas9 detection. (B) The detailed steps of RCA-assisted CRISPR/Cas9 detection. Step 1: miRNA-padlock probe (PP) ligation; Step 2: Rolling circular amplification (RCA) reaction; Step 3: Cas9/sgRNA cleavage and fluorescence detection.

## 2.3 | Animals, parasites, and sample collection

In the present study, a total of 154 animals were used. These animals include 74 rabbits, 77 mice, and 3 dogs. All animals were procured from the Laboratory Animal Center of Lanzhou Veterinary Research Institute and housed in specific-pathogen-free (SPF) facilities. *T. pisiformis* cysticerci were obtained from naturally infected rabbits by an abattoir in Henan province, China. To collect a sufficient number of *T. pisiformis* eggs, 3 male dogs (3 months old) were experimentally infected with 20 *T. pisiformis* cysticerci. At 50 days post-infection (dpi), eggs were collected from the feces of the infected dogs.

74 New Zealand white rabbits were randomly divided into two groups: an infection group (31 rabbits) and a control group (43 rabbits). In the infection group, each rabbit was orally administered 1000 mature eggs of *T. pisiformis*. In the control group, each rabbit received an equal volume of phosphate buffered saline (PBS). Plasma samples from the rabbits were collected at different intervals on days 0, 7, 14, 15, 30, 45, 60, 90, and 120 dpi. At 120 dpi (experimental end point), the rabbits were necropsied, and the number of cysticerci was analyzed.

*E. multilocularis* protoscolices used in the present study were isolated from Mongolian gerbils within the animal house of Lanzhou Veterinary Research Institute.<sup>42</sup> 77 male BALB/c mice (6–8 weeks old) were randomly assigned to two groups: an infection group (38 mice) and a control group (39 mice). In the infection group, each mouse was intraperitoneally infected with 1000 protoscolices. In the control group, each mouse received an equivalent volume of PBS. Plasma samples from all mice were collected at 0, 7, 14, 15, 30, 60, and 90 dpi. At 90 dpi (experimental end point), the mice were euthanized, and the weight of the cysts was analyzed.

## 2.4 | miRNA isolation, reverse transcription, and qPCR

After the blood sample collection, the miRNA was immediately isolated using an EasyPure miRNA Kit (TransGen, Beijing, China) according to the manufacturer's instructions. The isolated miRNA was then divided into two parts: one part was stored at  $-80^{\circ}\text{C}$  for the RCA-assisted CRISPR/Cas9 assay, while the other part was subjected to reverse transcription for qPCR analysis.

Two methods were employed for miRNA reverse transcription. In the poly (A) method, RNAs were reverse transcribed into cDNA using the Mir-XTM miRNA First Strand Synthesis Kit (Clontech, Mountain View, CA, USA). As for the stem-loop method, first-strand cDNA

was synthesized using the miRNA First Strand cDNA Synthesis Kit (by stem-loop) (Vazyme, Nanjing, China).

qPCR analysis was conducted using  $2\times$  Universal Blue SYBR Green qPCR Master Mix (Servicebio, Wuhan, China). Each qPCR reaction was prepared in a  $10\mu\text{L}$  volume, consisting of  $5\mu\text{L}$  of qPCR master mix,  $1\mu\text{L}$  of cDNA template,  $0.2\mu\text{L}$  of forward primer ( $10\mu\text{M}$ ),  $0.2\mu\text{L}$  of reverse primer ( $10\mu\text{M}$ ), and  $3.6\mu\text{L}$  of nuclease-free water. The qPCR analysis was carried out on an ABI 7500 thermocycler (Thermo Fisher Scientific, Waltham, MA, USA) with an initial denaturation at  $95^{\circ}\text{C}$  for 30 seconds, followed by 40 cycles at  $95^{\circ}\text{C}$  for 10 seconds, and  $60^{\circ}\text{C}$  for 30 seconds. Cel-miR-39-3p served as the exogenous control. The  $2^{-\Delta\Delta\text{Ct}}$  method was used for analyzing miRNA expression, and each reaction was performed in triplicate.

## 2.5 | Ligation reaction

The ligation reaction was conducted using  $3\mu\text{L}$  PP,  $3\mu\text{L}$  miRNA,  $0.5\mu\text{L}$  HiFi Taq DNA ligase (New England Biolabs, Inc., Ipswich, MA, USA),  $1\mu\text{L}$   $5\times$  ligase buffer, and  $2.5\mu\text{L}$  nuclease-free water at  $37^{\circ}\text{C}$  for 15 min.

## 2.6 | RCA reaction

The  $20\mu\text{L}$  RCA reaction system contained  $10\mu\text{L}$  ligation products,  $0.5\mu\text{L}$  phi29 DNA polymerase ( $10000\text{U}/\text{mL}$ , New England Biolabs, Inc.),  $2\mu\text{L}$   $10\times$  reaction buffer,  $2\mu\text{L}$  dNTP ( $2.5\text{mM}$ ), and  $5.5\mu\text{L}$  nuclease-free water. The reaction mixture was incubated at  $37^{\circ}\text{C}$  for 1 h.

## 2.7 | Cas9 cleavage reaction and fluorescence measurement

The RCA product and  $10\mu\text{L}$  TP ( $10\mu\text{M}$ ) were mixed and incubated at room temperature for 30 min to form double-stranded products. Subsequently, a  $20\mu\text{L}$  Cas9/sgRNA mixture was incubated with the double-stranded complex for 30 min in the dark. The fluorescence intensity (FI) was detected at 510 to 600 nm using a Varioskan™ LUX microplate reader (ThermoFisher Scientific).

## 2.8 | Agarose gel electrophoresis

The agarose gel experiments were conducted using 3% and 1% agarose gel at 100V for 30 min. Images were captured using a BIO-RAD Gel Doc XR imaging system (Hercules, CA, USA).



## 2.9 | Multiple sequence alignment analysis

The mature sequences of let-7 from different species were obtained from the miRBase database (<https://www.mirbase.org>), including cestodes (*E. granulosus*, *E. multilocularis*, *T. solium*, and *T. pisiformis*), nematodes (*Ascaris suum*), trematodes (*S. japonicum*), and mammals (*Homo sapiens*, *Ovis aries*, and *Oryctolagus cuniculus*). Multiple sequence alignment was performed using Clustal X software (version 2.1).

## 2.10 | Analytical sensitivity of qPCR, RCA, and RCA-assisted CRISPR/Cas9 assay

A series of miRNA dilutions of the let-7-5p standard was prepared, corresponding to concentrations of 10  $\mu$ M, 1  $\mu$ M, 100 nM, 10 nM, 1 nM, 100 pM, 10 pM, 1 pM, 100 fM, 10 fM, 1 fM, 100 aM, 10 aM, and 1 aM. The levels of let-7-5p were assessed using qPCR, RCA, and RCA-assisted CRISPR/Cas9, respectively. Three biological replicates were established for each sample.

## 2.11 | Analytical specificity of qPCR, RCA, and RCA-assisted CRISPR/Cas9 assay

Let-7 standards from different species, including *O. cuniculus* (ocu-let-7-5p), *A. suum* (asu-let-7-5p), *S. japonicum* (sja-let-7-5p), and *T. pisiformis* cysticercus (tpi-let-7-5p), were detected using poly(A)-tailing RT-qPCR, stem-loop RT-qPCR, RCA, and the RCA-assisted CRISPR/Cas9 methods, respectively. The specificity of RCA-assisted CRISPR/Cas9 detection for tpi-let-7-5p was compared with other methods.

## 2.12 | Diagnostic performance of RCA-assisted CRISPR/Cas9 assay

The levels of let-7-5p in blood samples from 74 rabbits (including 43 healthy rabbits and 31 *T. pisiformis* experimentally infected rabbits) and 77 mice (including 39 healthy mice and 38 *E. multilocularis* experimentally infected mice) were tested using the RCA-assisted CRISPR/Cas9 assay.

## 2.13 | Enzyme-linked immunosorbent assay (ELISA)

96-well plates were coated overnight at 4°C with 100  $\mu$ L/well of excretory/secretory product (ESP) from *T.*

*pisiformis* cysticercus diluted to 2.5  $\mu$ g/mL in carbonate buffer solution (CBS). All the following steps were performed at room temperature. After washing three times for 5 min with PBST, the wells were blocked for 2 h with 100  $\mu$ L/well of 5% bovine serum albumin. The plates were washed and incubated for 1 h with rabbit sera diluted 1:200 in PBST (100  $\mu$ L/well). After washing, the wells were incubated for 1 h with HRP goat anti-rabbit IgG (H + L) (1:5000; Biodragon, China). After a final washing, wells were incubated for 15 min in the dark with 100  $\mu$ L 3, 3', 5, 5'-tetramethylbenzidine (TMB) substrate. The reaction was stopped by addition of 100  $\mu$ L of 2 M H<sub>2</sub>SO<sub>4</sub>. The optical density (OD) of each well at 450 nm was measured on a Varioskan™ LUX microplate reader (ThermoFisher Scientific). All serum samples were tested in duplicate.

*E. multilocularis* hydatid cyst fluid was used as a coated antigen to detect serum antibody levels in mice by the indirect ELISA method described above.

## 2.14 | Data analysis

Comparative analysis was conducted using the Student's *t*-test. Pearson's correlation coefficient (*r*) was employed to assess the correlation between plasma levels of let-7-5p and the number of cysticerci or the weight of cysts. Statistical analysis was performed using GraphPad Prism version 8 (GraphPad Software, San Diego, CA, USA). A significance level of *p* < .05 was considered statistically significant. The diagnostic sensitivity and specificity were assessed using a receiver operating characteristic (ROC) curve. The optimal cut-off value for the method was determined using the Youden index.<sup>43</sup>

## 3 | RESULTS

### 3.1 | Principle and design for RCA-assisted CRISPR/Cas9

RCA-assisted CRISPR/Cas9 based on let-7-5p consists of three steps: miRNA-PP ligation (Step 1), RCA (Step 2), and CRISPR/Cas9 cleavage (Step 3) (Figure 1). First, a PP with a PAM motif hybridizes with the target miRNA, triggering the ligation of the 5' and 3' terminals of the PP by high-fidelity HiFi Taq DNA ligase. The resulting circular PP acts as a template to mediate the RCA reaction, forming ssDNA RCA amplicons in the presence of phi29 DNA polymerase. Subsequently, the TP (FAM at the 5' terminal and BHQ-1 at the 3' terminal), complementary to the target, is added. It hybridizes with the repetitive target regions of ssDNA RCA amplicons, forming a long dsDNA assembly. The Cas9/sgRNA complex specifically

cleaves the dsDNA assembly adjacent to the PAM motif. Fluorescence is emitted from the digested TP, observed either by the naked eye or by a fluorescence reader.

### 3.2 | Padlock probes optimization and intermediate product analysis

The efficiency of the padlock cyclization reaction and subsequent RCA reaction depends on the secondary structure of PP. To establish the RCA-assisted CRISPR/Cas9 detection method based on let-7-5p, four PPs with different structures were designed using RNA structure (<http://rna.urmc.rochester.edu/RNAstructure.html>). These included PP1 without secondary structure (Figure S1), PP2 with secondary structure in the middle (Figure S2), PP3 with secondary structure at the 3' end (Figure S3), and PP4 with secondary structure at the 5' end (Figure S4). The corresponding fluorescence intensity (FI) of the four PPs was measured. Results indicated that the FI of PP1

was significantly higher than that of the other three PPs (Figure 2A,B,  $p < .01$ ). Hence, PP1 was selected as the optimal padlock probe for the RCA assisted CRISPR/Cas9 method.

To analyze the generation of intermediate products, the ligation product and the RCA product were subjected to agarose gel electrophoresis. The results revealed that the size of let-7-5p was about 22 bp (lane 1), PP1 was about 75 bp (lane 2), and the ligation product was about 97 bp (lane 3) (Figure 2C). This indicated successful ligation between let-7-5p and PP1. The RCA product exhibited a prominent band at the sample addition hole (Figure 2D, lane 4), suggesting that the amplification products reached a magnitude of  $10^4$ .

### 3.3 | Analytical performance

To determine the sensitivity of the RCA-assisted CRISPR/Cas9 assay, the correlation between let-7-5p concentration and FI was initially explored. As illustrated in Figure 3A,

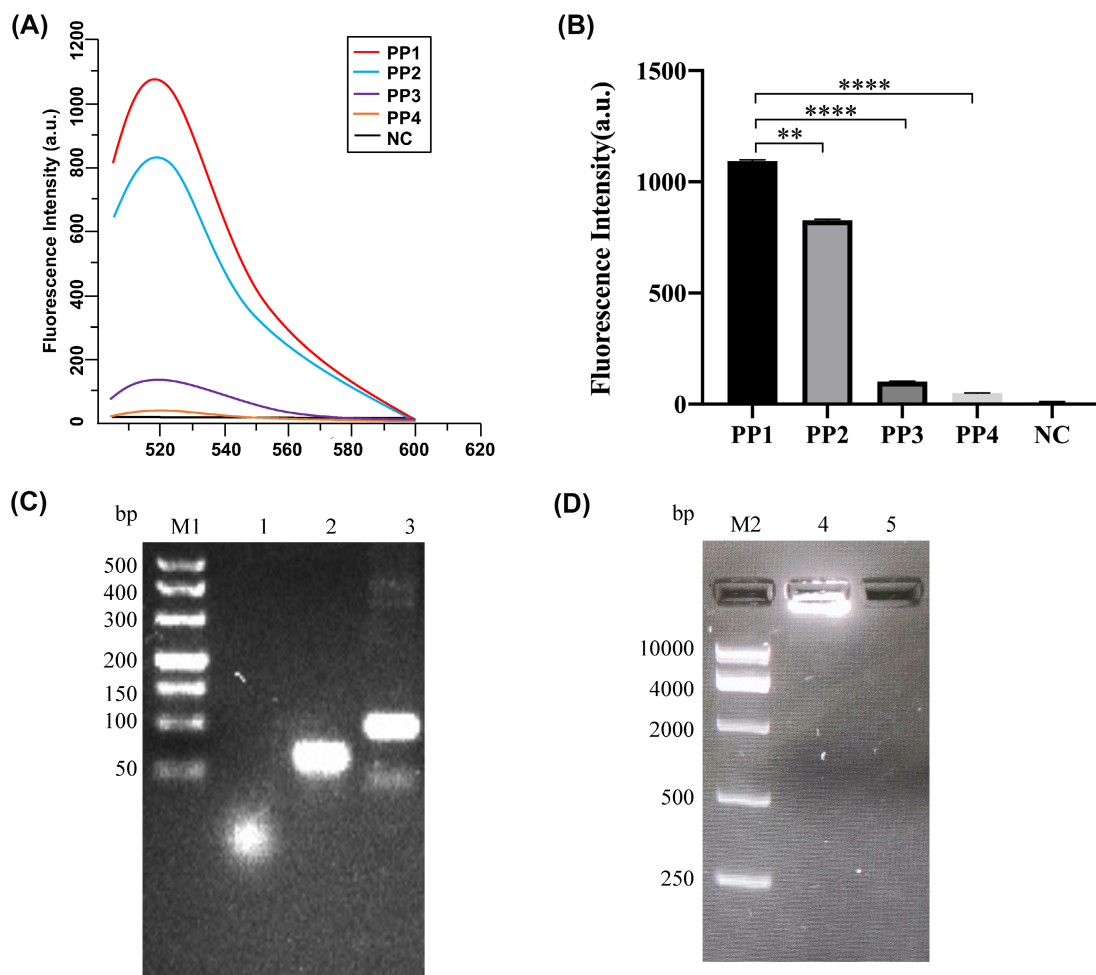


**FIGURE 2** Intermediate product analysis of RCA. (A) FI analysis of padlock probes (PP). (B) Comparative analysis of FI in the four PPs. (C) 3% agarose gel electrophoresis analysis of the ligation product. (D) 1% agarose gel electrophoresis analysis of the RCA product. M1: GL DNA marker 500 bp; 1: tpi-let-7-5p; 2: PP1; 3: ligation product; M2: DL 10000 DNA Marker; 4: RCA product; 5: Negative control. \*\* $p < .01$ , \*\*\*\* $p < .0001$ , compared with the PP1 group.

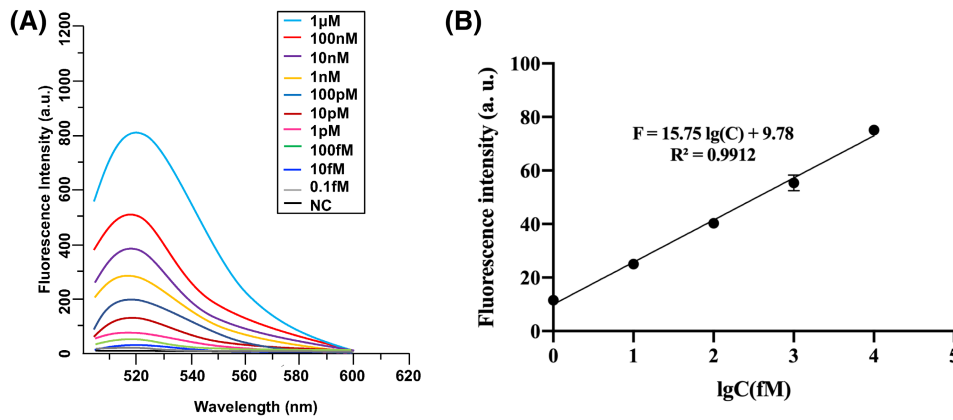


FIGURE 3 Correlation analysis between FI and tpi-let-7-5p. (A) FI of different concentrations of let-7-5p. (B) Linear analysis between FI and tpi-let-7-5p concentration (lgC).

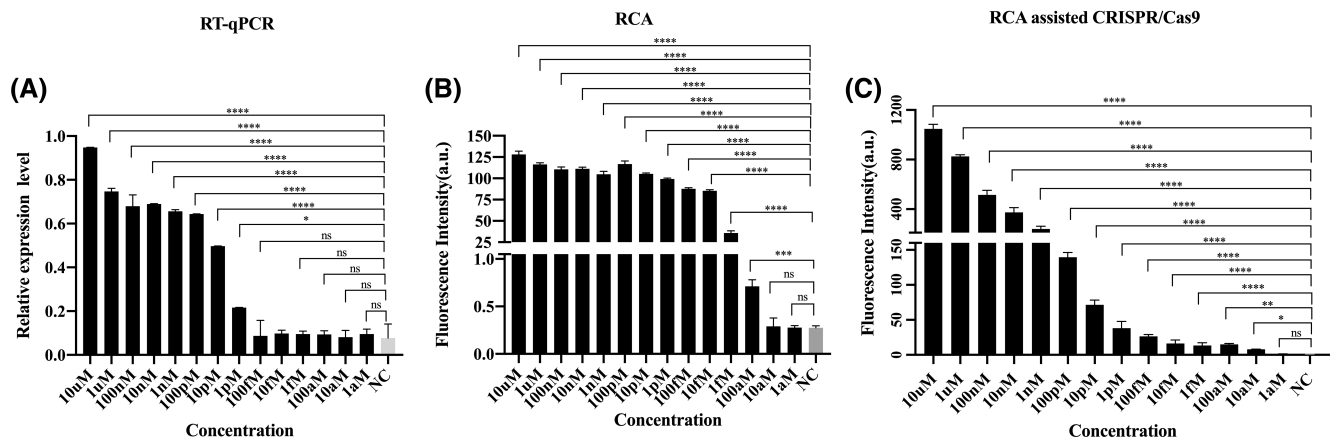


FIGURE 4 The sensitivity analysis of RT-qPCR, RCA, and RCA-assisted CRISPR/Cas9 methods using the let-7-5p standard. (A) Serial dilutions of the let-7-5p standard were detected by RT-qPCR. (B) Serial dilutions of the let-7-5p standard were detected by RCA. (C) Serial dilutions of the let-7-5p standard were detected by an RCA-assisted CRISPR/Cas9 assay. Data are presented as mean  $\pm$  SD. *p*-values were analyzed using the Student's *t*-test; <sup>ns</sup>*p* > .05, \**p* < .05, \*\**p* < .01, \*\*\**p* < .001, \*\*\*\**p* < .0001, compared with the NC group.

the FI increased gradually as the let-7-5p concentration increased from 0.1 fM to 0.1 μM, indicating a strong correlation between the concentration of let-7-5p and the fluorescent signal. Furthermore, a robust linear relationship between FI and let-7 concentration was observed, represented by the regression equation  $F = 15.75 \lg(C) + 9.78$  ( $R^2 = .9912$ ) (Figure 3B).

By employing serial dilutions of let-7-5p, it was found that the limits of detection (LODs) for let-7-5p were 1 pM for qPCR, 100 aM for RCA, and 10 aM for the RCA-assisted CRISPR/Cas9 assay (Figure 4). These results suggest that the sensitivity of the RCA-assisted CRISPR/Cas9 assay surpasses that of the qPCR and RCA methods. This indicates an enhanced capability of the RCA-assisted CRISPR/Cas9 detection method in identifying low levels of let-7-5p.

To evaluate the specificity of the RCA-assisted CRISPR/Cas9 assay for let-7 detection, a sequence conservation analysis of let-7 from different species was performed

using the multi-sequence alignment software ClustalX (version 2.1) (Figure 5). The results revealed that cestodes (*E. granulosus*, *E. multilocularis*, *T. solium*, and *T. pisiiformis*) share identical let-7 sequences, unlike nematodes (*A. suum*), trematodes (*S. japonicum*), and mammals (*H. sapiens*, *O. aries*, and *O. cuniculus*), indicating highly conserved sequences of let-7-5p among cestodes.

Given that qPCR serves as a gold standard method for miRNA quantification, we compared the specificity of poly(A)-tailing RT-qPCR, stem-loop RT-qPCR, and RCA-assisted CRISPR/Cas9 assays for detecting let-7 standards from four different species (tpi-let-7-5p, ocu-let-7c-5p, asu-let-7-5p, and sja-let-7-5p). The findings revealed that let-7 from four different species could not be distinguished by poly(A)-tailing RT-qPCR or RCA (Figure 6A,C). However, they could be differentiated using stem-loop RT-qPCR (Figure 6B).

Compared to poly(A)-tailing RT-qPCR, stem-loop RT-qPCR significantly improved the specificity of the qPCR

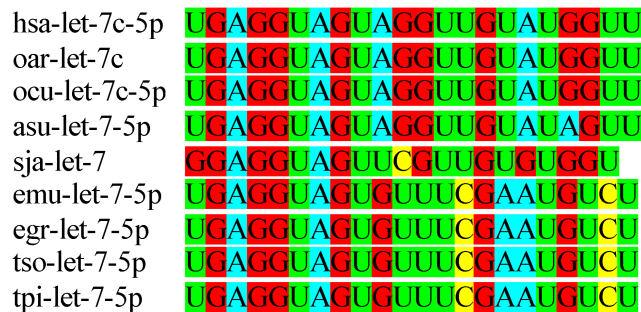


**FIGURE 5** Alignment of the let-7 sequence from different species. has: *Homo sapiens*; oar: *Ovis aries*; ocu: *Oryctolagus cuniculus*; asu: *Ascaris suum*; sja: *Schistosomiasis japonica*; emu: *Echinococcus multilocularis*; egr: *Echinococcus granulosus*; tso: *Taenia solium*; tpi: *Taenia pisiformis*.

reaction. However, the fold change of let-7 between cestodes and let-7 from other species was significantly lower ( $<0.5$  times, [Figure 6B](#)) than that of the RCA-assisted CRISPR/Cas9 method (approximately 48 times, [Figure 6D](#)). Moreover, the RCA-assisted CRISPR/Cas9 method can significantly distinguish let-7 family members with single base differences (such as ocu-let-7-5p and asu-let-7-5p) when compared to qPCR and RCA.

Taken together, these analytical performances suggest that RCA-assisted CRISPR/Cas9 based on cestode-derived let-7-5p is a promising molecular method for detecting metacestodiasis, demonstrating remarkable analytical sensitivity and specificity.

### 3.4 | Diagnostic performance

To assess the diagnostic potential of the RCA-assisted CRISPR/Cas9 assay for *T. pisiformis* infection, a total of 74 blood samples were collected, comprising 43 from healthy rabbits and 31 from *T. pisiformis* cysticercus-infected rabbits. The levels of let-7-5p were detected in those samples. As shown in [Figure 7A](#), a statistically significant difference in the fold change of *T. pisiformis* cysticercus-infected rabbits compared to healthy rabbits was observed ( $p < .0001$ ). The ROC curve analysis revealed an optimal cut-off value of 2.13. Accordingly, one out of 43 healthy rabbits exhibited a fold change above the cut-off value, indicating a specificity of 97.67% (87.94%–99.88%, 95% CI) ([Figure 7B](#)). All parasitologically confirmed infected rabbits were considered positive, yielding a sensitivity of 100% (88.97%–100%, 95% CI). The area under the ROC curve (AUC) assesses the ability of the test to discriminate between healthy and diseased individuals. An AUC of 1 represents a perfect test, while an AUC of 0.5 indicates a test without the ability to differentiate diseased individuals from healthy individuals.<sup>44</sup> In this test, the AUC was

0.9992 (99.68%–100%, 95% CI), suggesting excellent diagnostic performance of the RCA-assisted CRISPR/Cas9 based on tpi-let-7-5p for *T. pisiformis* cysticercosis. While the ELISA results showed that sensitivity and specificity were 87.4% and 81.4% in detecting 74 sera of rabbits from *T. pisiformis* infection, respectively ([Figure 7C](#)).

To evaluate the diagnostic performance of the RCA-assisted CRISPR/Cas9 method for *E. multilocularis* infection, the levels of let-7-5p were detected in 39 healthy and 38 *E. multilocularis*-infected mice. A statistically significant difference was observed in the fold change of *E. multilocularis*-infected mice compared to healthy mice ([Figure 7D](#),  $p < .0001$ ). The positive samples showed an average fold change value of 4.32, while the negative ones had an average fold change value of 0.96. The determined optimal cut-off value of this method was 2.46, yielding sensitivity and specificity of 100% (90.82%–100%, 95% CI) and 100% (91.03%–100%, 95% CI), respectively ([Figure 7E](#)). The AUC was 1, indicating robust potential clinical utility of parasite-derived let-7 as a diagnostic target for AE. The ELISA results with cyst fluid antigen as coated antigen showed that sensitivity and specificity were 92.11% and 84.62% in detecting 77 sera of mice infected with *E. multilocularis*, respectively ([Figure 7F](#)).

To evaluate the cross-reactivity of the RCA-assisted CRISPR/Cas9 assay between different species of let-7-5p, different species of let-7-5p were added to *O. aries* blood, and the levels of let-7-5p were detected. The results showed that this method could only detect the high expression of let-7-5p in blood samples containing egr-let-7-5p, but there was no cross-reaction with let-7 in other species ([Figure 8](#)).

Taken together, the RCA-assisted CRISPR/Cas9 assay based on let-7-5p has demonstrated high sensitivity and specificity in diagnosing metacestodiasis.

### 3.5 | Dynamic changes of let-7-5p in animal plasma during metacestode infection

To monitor the dynamic changes of tpi-let-7-5p in plasma of both healthy rabbits and *T. pisiformis* cysticercus-infected rabbits, the expression of tpi-let-7-5p in plasma samples was assessed at different time points using poly(A)-tailing RT-qPCR and RCA-assisted CRISPR/Cas9 assays, respectively. The results of poly(A)-tailing RT-qPCR indicated a significant upregulation of tpi-let-7-5p in the plasma of *T. pisiformis* cysticercus-infected rabbits at 60 dpi, but no statistically significant changes were observed at 7, 14, 15, 30, 45, 90, or 120 dpi ([Figure 9A](#),  $p < .05$ ). Conversely, the RCA-assisted CRISPR/Cas9 assay demonstrated a gradual increase of tpi-let-7-5p from 15 dpi, which peaked at 60 dpi and persisted until 120 dpi ([Figure 9B](#)).



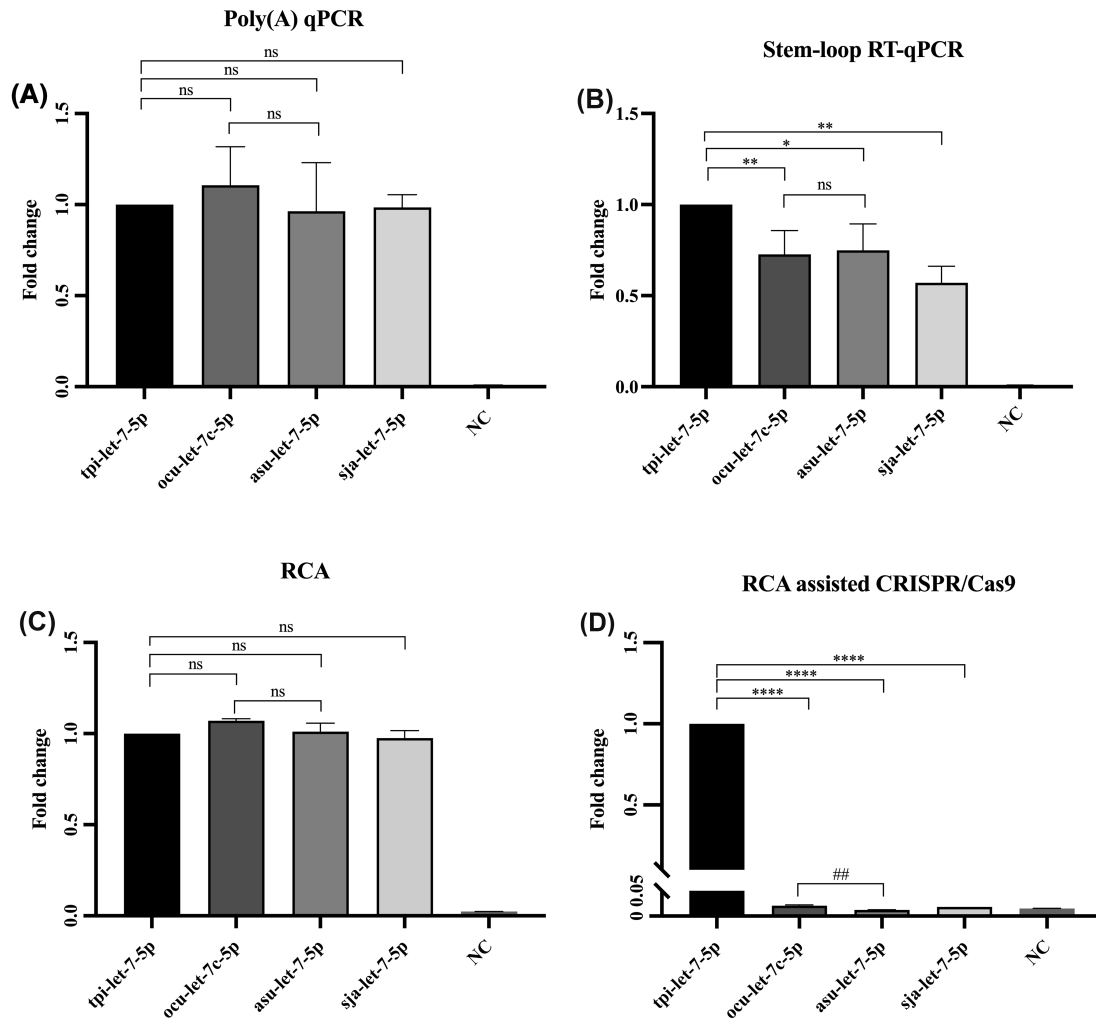


**FIGURE 6** The specificity analysis of poly(A)-tailing RT-qPCR, stem-loop RT-qPCR, RCA, and RCA-assisted CRISPR/Cas9 methods using let-7-5p from four species. (A) The specificity analysis of poly(A)-tailing RT-qPCR. (B) The specificity analysis of stem-loop RT-qPCR. (C) The specificity analysis of RCA. (D) The specificity analysis of the RCA-assisted CRISPR/Cas9 method. <sup>ns</sup> $p > .05$ , <sup>\*</sup> $p < .05$ , <sup>\*\*</sup> $p < .01$ , <sup>\*\*\*\*</sup> $p < .0001$  vs. tpi-let-7-5p. <sup>##</sup> $p < .01$  vs. ocu-let-7-5p.

Additionally, we investigated the dynamic changes of emu-let-7-5p in the plasma of healthy mice and *E. multilocularis*-infected mice. The results of poly(A)-tailing RT-qPCR indicated a significant upregulation of emu-let-7-5p in the plasma of *E. multilocularis*-infected mice at 30 and 60 dpi, but with no statistically significant changes observed at 7, 14, 15 or 90 dpi (Figure 9C,  $p < .05$ ). The results of the RCA-assisted CRISPR/Cas9 assay showed that emu-let-7-5p gradually increased from 15 dpi and persisted until 90 dpi (Figure 9D). These results indicate that the RCA-assisted CRISPR/Cas9 assay based on cestode-derived let-7-5p can be used for the diagnosis of metacestodiasis, especially for early detection at 15 dpi.

### 3.6 | Correlations between the level of let-7-5p in plasma and the infected number of cysticerci or weight of cysts

Correlation analysis revealed a positive correlation between the level of tpi-let-7-5p in the plasma of rabbits infected with *T. pisiformis* and the number of cysticerci (Figure 10A,  $r = .7428$ ,  $p < .0001$ ). Additionally, in the plasma of mice infected with *E. multilocularis*, a significant positive correlation was observed between the level of emu-let-7-5p and the weight of cysts (Figure 10B,  $r = 0.9515$ ,  $p < .0001$ ). Noticeably, the RCA-assisted CRISPR/Cas9 method demonstrated the ability to detect at least three cysticerci infections (Figure 10A).

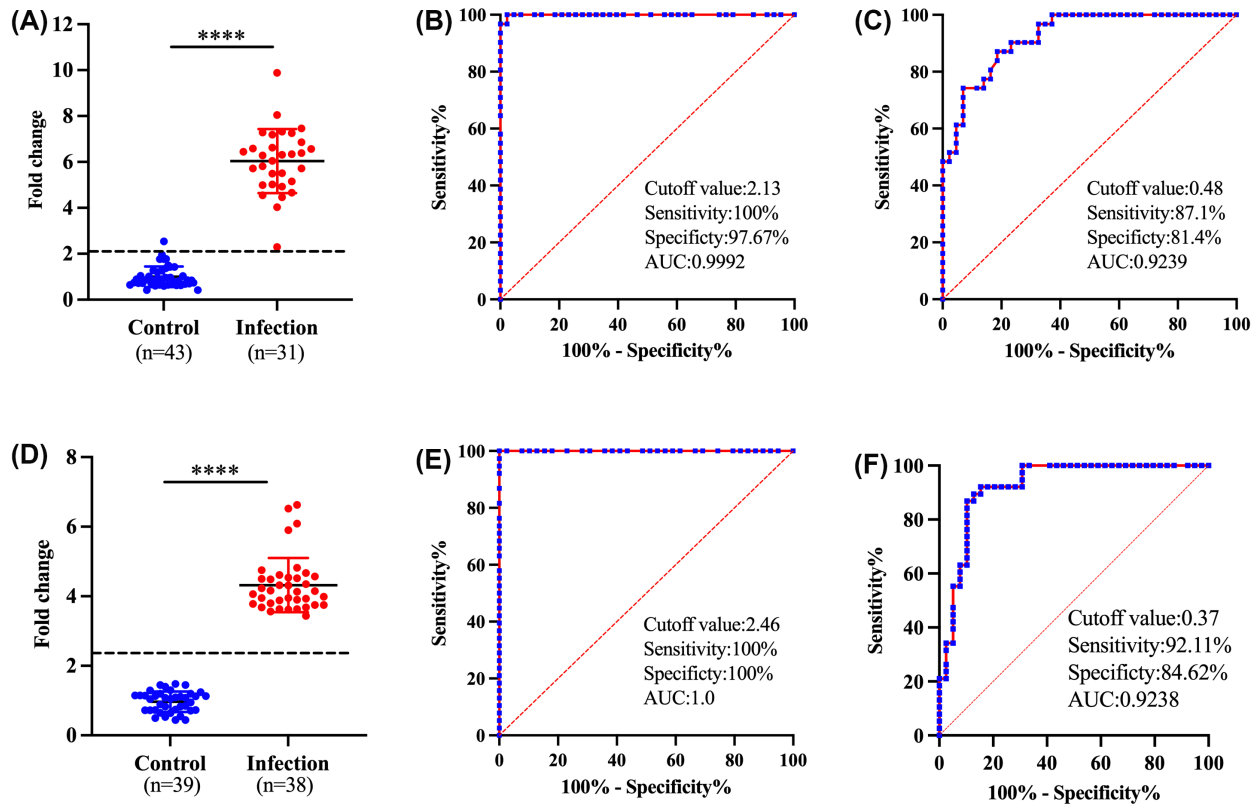


**FIGURE 7** Diagnostic performance analysis of RCA-assisted CRISPR/Cas9 methods. (A) Scatter plot of parasite-derived let-7-5p for discriminating the *T. pisiformis*-infected rabbits from the control group. (B) ROC curves and AUC analysis of tpi-let-7-5p for rabbit cysticercosis diagnosis by the RCA-assisted CRISPR/Cas9 method. (C) ROC curves and AUC analysis for rabbit cysticercosis diagnosis by ELISA. (D) Scatter plot of parasite-derived let-7-5p for discriminating *E. multilocularis*-infected mice from the control group. (E) ROC curves and AUC analysis of emu-let-7-5p for AE diagnosis by RCA-assisted CRISPR/Cas9 method. (F) ROC curves and AUC analysis for AE diagnosis by ELISA. \*\*\*\* $p < .0001$ , compared with the control group.

## 4 | DISCUSSION

Accurate and specific detection of parasite-specific molecules is pivotal for preventing and controlling parasitic diseases.<sup>15</sup> In the present study, we established an isothermal amplification method for detecting parasite-derived miRNA let-7-5p, termed the RCA-assisted CRISPR/Cas9 assay based on let-7-5p, and demonstrated its application potential for the diagnosis of metacestodiasis, particularly in early infection stages. This method can be performed in the temperature range of 25–37°C and does not require sophisticated instruments (Figure 1). The entire reaction process takes no more than 2.5 h, and the fluorescence can be easily observed by the naked eye under ultraviolet excitation (Table 1 and Figure 1) or via a portable fluorescence detector.<sup>45</sup> Moreover, the assay is also cost-effective, with an estimated cost of \$1.92 per test (Table S2). Hence, the let-7-based RCA-assisted CRISPR/Cas9 assay is suitable for field detection without the need for a laboratory setting.

Previous studies have shown that high-throughput sequencing and modified stem-loop RT-qPCR can detect

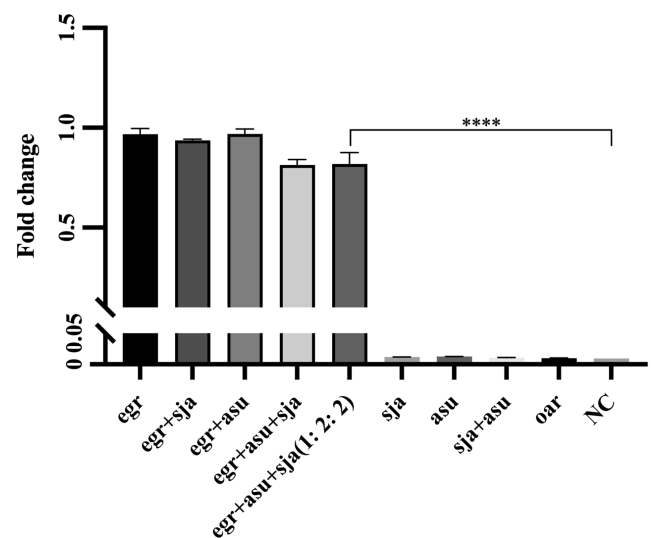


**FIGURE 8** Analysis of cross-reactivity between different species of let-7-5p using the RCA-assisted CRISPR/Cas9 method. egr: *Echinococcus granulosus*; asu: *Ascaris suum*; sja: *Schistosomiasis japonica*; oar: *Ovis aries*. egr + asu + sja (1: 2: 2) indicates the concentration ratio of egr, asu, and sja is 1: 2: 2. \*\*\*\* $p < .0001$ , compared with NC group.

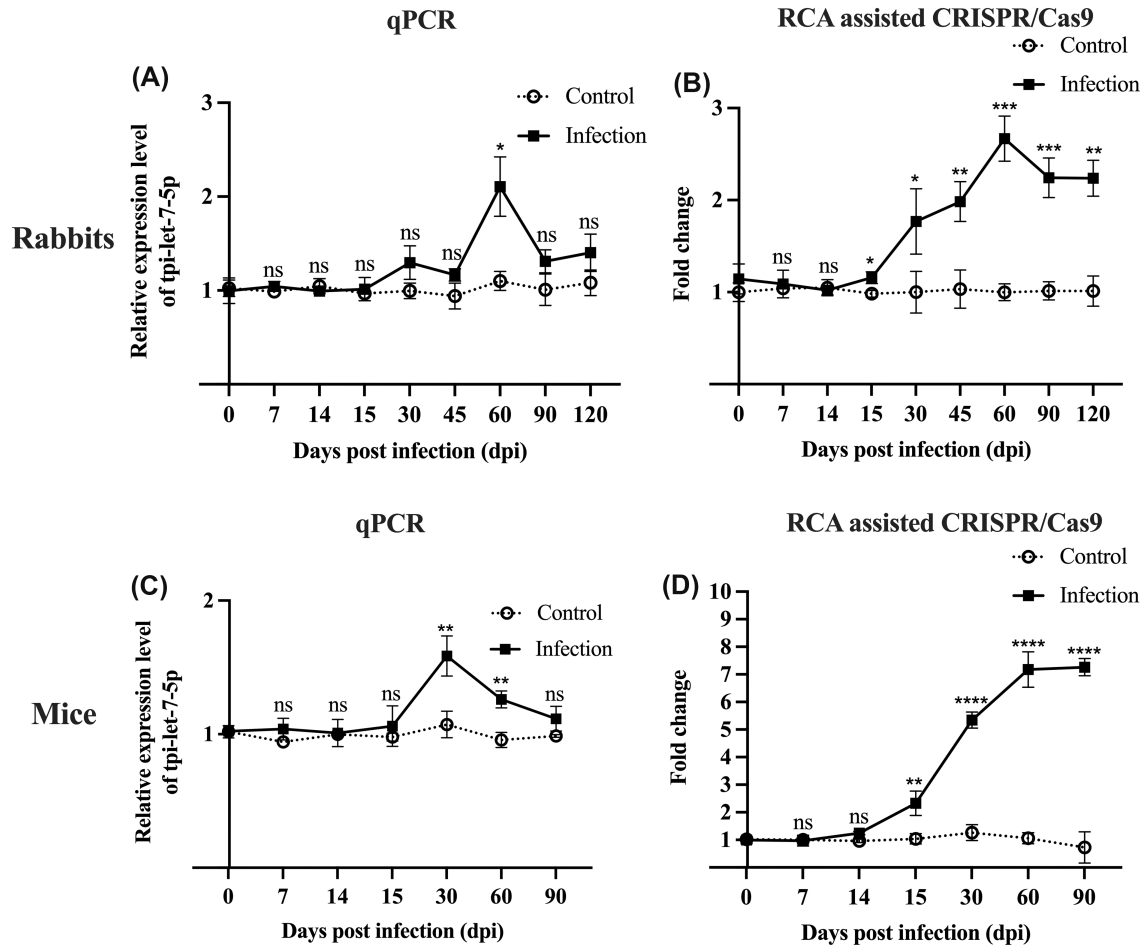


**FIGURE 9** Dynamic changes of let-7-5p levels in plasma. (A) Detection of let-7-5p in the plasma of healthy and infected rabbits by poly(A)-tailing RT-qPCR. miRNA was normalized by cel-miR-39-3p. (B) Detection of let-7-5p in the plasma of healthy and infected rabbits by RCA-assisted CRISPR/Cas9. The fluorescent signal was normalized by the no-template control (NTC). (C) Detection of let-7-5p in the plasma of healthy and infected mice by poly(A)-tailing RT-qPCR. (D) Detection of let-7-5p in the plasma of healthy and infected mice by RCA-assisted CRISPR/Cas9.

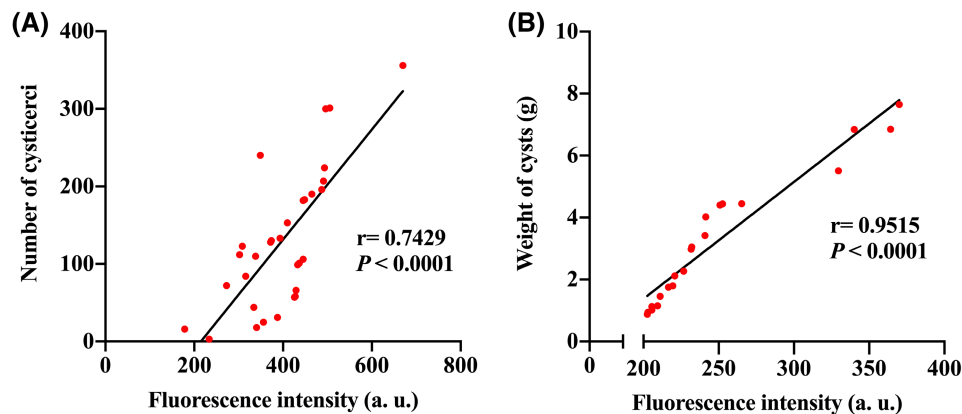


**FIGURE 10** Correlations between plasma levels of let-7-5p and the number of cysticerci or weight of cysts, using Pearson's correlation coefficient. (A) Correlation between plasma levels of let-7-5p and the number of cysticerci in rabbits. (B) Correlation between plasma levels of let-7-5p and the weight of cysts in mice.

TABLE 1 Comparison of CRISPR/Cas9 with other miRNA detection methods.

Detection methods	Reverse transcription step	SBD	Sensitivity	Assay time	Cost per test	Reference
Modified stem-loop RT-qPCR	Yes	Yes	High	>4 h	N/A	[46]
RT-qPCR	Yes	N/A	miR-21-5p: 7.4 fM	>2 h	N/A	[47]
Rolling circle amplification (RCA)	No	Yes	let-7: 2.5 fM	80 min	N/A	[32]
Cas12a-TCA	No	Yes	miR-21: 8 fM	7 h	\$ 2.7	[48]
Branched RCA and CRISPR-Cas12a (BRCAcas)	No	Yes	miR-21: 0.87 fM	5.5 h	\$ 3.7	[38]
RCA-CRISPR-split-HRP (RCH)	No	Yes	Let-7a: 1 fM	<4 h	\$ 1.73	[49]
CRISPR/Cas 13a-triggered RCA-DNAzyme	No	Yes	miR-10b: 1 fM	5.2 h	N/A	[50]
CRISPR/Cas 13a powered portable	No	N/A	miR-17: $1 \times 10^{-15}$ M	N/A	N/A	[51]
CRISPR/Cas9-assisted garland RCA	No	N/A	miR-326: 3.45 fM	2.5 h	N/A	[40]
let-7-based RCA-assisted CRISPR/Cas9	No	Yes	let-7: 10 aM	<2.5 h	\$ 1.92	This work

Abbreviations: N/A, not available; RCA, rolling circle amplification; SBD, single base discrimination.

single-base differences among let-7 family members<sup>46,52</sup> The present study also demonstrated that stem-loop qPCR can distinguish distinct let-7 family members (Figure 6A), which is consistent with the previous report.<sup>52</sup> However, this method requires different stem-loop primers and forward qPCR primers for various miRNAs, along with the preparation of a specific reverse transcription system before qPCR detection. Consequently, this approach is time-consuming (more than 4 h),<sup>53</sup> complex, and requires trained technicians. As a result, these limitations hinder its application in the rapid field detection of pathogens.

Utilizing branch-rolling circle amplification and CRISPR/Cas12a, a sensitive and specific serum miRNA detection method was established, featuring a LOD of 0.87 fM for miR-21. This method holds promise for diagnosing and screening the prognosis of colorectal cancer patients.<sup>38</sup> Furthermore, a highly specific RCA-assisted CRISPR/Cas9 detection method was developed. Not only does it possess single-base recognition characteristics and a LOD of 90 fM for miR-21, but it is also applicable in diagnosing patients with non-small-cell lung cancer.<sup>41</sup> The present study highlights that the RCA-assisted CRISPR/Cas9 method based on let-7-5p exhibits excellent specificity, enabling the significant differentiation of let-7 family members with single-base differences. The high specificity of this method is mainly due to two factors: firstly, HiFi Taq DNA ligase demonstrates enhanced discrimination between correct and mismatched base pairs at ligation junctions, enabling differentiation of single-base differences at the terminal of 3' or 5'. Secondly, Cas9 nucleases accurately cleave hybridized double strands adjacent to the PAM domain. Additionally, by integrating

the advantages of RCA, CRISPR/dCas9, and horseradish peroxidase (HRP) technologies, a novel, cost-effective, and highly efficient miRNA detection method was established, achieving a LOD of 1 fM for let-7a.<sup>49</sup>

In the present study, the let-7-based RCA-assisted CRISPR/Cas9 method demonstrated higher sensitivity than traditional qPCR and RCA, with a LOD as low as 10 aM. Particularly in the detection of low-abundance samples such as miRNA, the sensitivity of the detection method holds great importance, especially in the early diagnosis of pathogen infections. Immediate intervention measures in the early stages play a crucial role in effectively preventing and controlling diseases.

Parasite-derived miRNAs offer significant potential as biomarkers for diagnosing infections in humans or animals. One study developed a stem-loop RT-qPCR assay based on *Echinococcus granulosus*-derived egr-miR-2a-3p, effectively distinguishing healthy subjects from cystic echinococcosis patients. ROC analysis revealed its good diagnostic value for cystic echinococcosis, with an AUC of 0.8176.<sup>17</sup> Another study identified two parasite-derived miRNAs, egr-miR-71 and egr-let-7, exclusively detected in the plasma of *E. granulosus*-infected individuals. Their expression levels significantly decreased at 3 and 6 months post-surgery, suggesting potential use as novel biomarkers for *E. granulosus* infection detection and post-surgery follow-up.<sup>15</sup> According to a recent report, three highly expressed parasite-derived miRNAs (egr-let-7-5p, egr-miR-71a-5p, and egr-miR-9-5p) were found to be upregulated in the serum of Cystic Echinococcosis (CE) patients when compared to the active CE patients. ROC analysis showed that the egr-let-7-5p can not only discriminate between healthy and CE patients (AUC=0.9170), but



it can also distinguish between active and inactive CE patients (AUC = 0.8024).<sup>23</sup> The present study demonstrated that the let-7-5p-based RCA-assisted CRISPR/Cas9 method effectively distinguished between healthy controls and metacestode-infected animals. The diagnostic sensitivity and specificity for rabbit cysticercosis were 100% and 97.67%, respectively, with an AUC of 0.9992. For *Echinococcus multilocularis* in mice, the diagnostic sensitivity and specificity were 100%, and the AUC was 1. Moreover, the let-7 sequence, being identical among cestodes, distinguishes them from mammals, nematodes, and trematodes using the RCA-assisted CRISPR/Cas9 assay. Therefore, the let-7-5p-based RCA-assisted CRISPR/Cas9 assay can be used as a universal diagnostic method for metacestodiasis.

Despite the advantages of this novel approach, it still has limitations. The experimental process involves three steps, which could potentially result in cross-contamination. Hence, future research should prioritize the development of a single-tube assay, aiming for reduced time and enhanced accuracy. Nevertheless, this novel method represents a new approach for detecting parasite-specific miRNA let-7 in the plasma of *T. pisiformis* cysticercus-infected rabbits and *E. multilocularis*-infected mice. It can also be adapted for detecting other metacestodes. Given the relatively low incidence of metacestode infections in humans, this method holds promise for the early diagnosis of human cysticercosis and echinococcosis. Its accuracy can be further enhanced by combining it with radiological technology.

#### AUTHOR CONTRIBUTIONS

Liqun Wang and Xuenong Luo conceived the idea for this study. Liqun Wang designed experiments and drafted the initial version of the manuscript. Guiting Pu and Tingli Liu assisted in performing the RT-qPCR experiments. Shanling Cao assisted in performing the ELISA. Liqun Wang, Hong Li, and Guoliang Chen collected the clinical samples. Liqun Wang and Hongbin Yan performed the data analyses. Liqun Wang and Tharheer Amuda drafted the final version of the manuscript. Xuenong Luo, Baoquan Fu, and Hong Yin revised and reviewed the final version of the manuscript. All authors read and approved the final manuscript. Xuenong Luo contributed to funding acquisition, supervision, writing review, and editing.

#### ACKNOWLEDGMENTS

This work was financially supported by the National Natural Science Foundation of China (32072889) and the National Key Research and Development Program of China (2023YFD1802401). We thank the scientific staff at the Instrument Center of Lanzhou Veterinary Research Institute for their technical assistance.












#### DISCLOSURES

The authors declare that no competing interests exist.

#### DATA AVAILABILITY STATEMENT

All relevant data are contained within this article and the [supplementary material](#).

#### ORCID

Liqun Wang  <https://orcid.org/0000-0003-2642-1017>  
 Guiting Pu  <https://orcid.org/0009-0008-0064-6465>  
 Tingli Liu  <https://orcid.org/0009-0006-5587-5500>  
 Guoliang Chen  <https://orcid.org/0000-0002-2844-6376>  
 Hong Li  <https://orcid.org/0009-0008-8397-4105>  
 Tharheer Oluwashola Amuda  <https://orcid.org/0000-0002-1987-0837>  
 Shanling Cao  <https://orcid.org/0009-0004-2420-585X>  
 Hongbin Yan  <https://orcid.org/0000-0002-8522-0875>  
 Hong Yin  <https://orcid.org/0000-0001-6404-7965>  
 Baoquan Fu  <https://orcid.org/0000-0002-3938-1336>  
 Xuenong Luo  <https://orcid.org/0000-0001-7457-2325>

#### REFERENCES

- Dixon MA, Winskill P, Harrison WE, et al. *Taenia solium* taeniasis/cysticercosis: from parasite biology and immunology to diagnosis and control. *Adv Parasitol*. 2021;112:133-217.
- Yang D, Yang G. Research progress on rabbit cysticercosis. *China Animal Husband Vet Med*. 2015;42:1015-1020.
- Hallal-Calleros C, Morales-Montor J, Orihuela-Trujillo A, et al. *Taenia pisiformis* cysticercosis induces decreased prolificacy and increased progesterone levels in rabbits. *Vet Parasitol*. 2016;229:50-53.
- Rosa DR, David AH, Emmanuel DG, et al. Decreased embryo implantation in rabbits infected with *taenia pisiformis*. *Parasitol Res*. 2022;121:3689-3692.
- Sezgin O, Altintaş E, Saritaş U, Sahin B. Hepatic alveolar echinococcosis: clinical and radiologic features and endoscopic management. *J Clin Gastroenterol*. 2005;39:160-167.
- Anthony B, Allen JT, Li YS, McManus DP. Hepatic stellate cells and parasite-induced liver fibrosis. *Parasit Vectors*. 2010;3:60.
- Gao CH, Wang JY, Shi F, et al. Field evaluation of an immunochromatographic test for diagnosis of cystic and alveolar echinococcosis. *Parasit Vectors*. 2018;1:311.
- Zhu GQ, Li L, Ohiolei JA, et al. A multiplex PCR assay for the simultaneous detection of *Taenia hydatigena*, *T. multiceps*, *T. pisiformis*, and *Dipylidium caninum* infections. *BMC Infect Dis*. 2019;19:854.
- Chen L, Yang D, Gu X, Peng X, Yang G. Evaluation of a novel dot-ELISA assay utilizing a recombinant protein for the effective diagnosis of *Taenia pisiformis* larval infections. *Vet Parasitol*. 2014;204:214-220.
- O'Brien J, Hayder H, Zayed Y, Peng C. Overview of microRNA biogenesis, mechanisms of actions, and circulation. *Front Endocrinol (Lausanne)*. 2018;9:402.
- Rojas-Pirela M, Andrade-Alviárez D, Medina L, et al. MicroRNAs: master regulators in host-parasitic protist interactions. *Open Biol*. 2022;12:210395.

12. MacLellan SA, MacAulay C, Lam S, et al. Pre-profiling factors influencing serum microRNA levels. *BMC Clin Pathol*. 2014;14:27.
13. Silva SS, Lopes C, Teixeira AL, Sousa MJC, Medeiros R. Forensic miRNA: potential biomarker for body fluids? *Forensic Sci Int Genet*. 2015;14:1-10.
14. Mu Y, Cai P, Olveda RM, Ross AG, Olveda DU, McManus DP. Parasite-derived circulating microRNAs as biomarkers for the detection of human *Schistosoma japonicum* infection. *Parasitology*. 2020;147:889-896.
15. Alizadeh Z, Mahami-Oskouei M, Spotin A, et al. Parasite-derived microRNAs in plasma as novel promising biomarkers for the early detection of hydatid cyst infection and post-surgery follow-up. *Acta Trop*. 2020;202:105255.
16. Hoy AM, Lundie RJ, Ivens A, et al. Parasite-derived microRNAs in host serum as novel biomarkers of helminth infection. *PLoS Negl Trop Dis*. 2014;8:e2701.
17. Karami MF, Beirovand M, Rafiei A, et al. Serum level of egr-miR-2a-3p as a potential diagnostic biomarker for cystic echinococcosis. *Acta Parasitol*. 2023;68:114-121.
18. Wang L, Liu T, Chen G, et al. Exosomal microRNA let-7-5p from *Taenia pisiformis* *Cysticercus* prompted macrophage to M2 polarization through inhibiting the expression of C/EBP  $\delta$ . *Microorganisms*. 2021;9:1403.
19. Chen G, Wang L, Liu T, et al. Identification and expression profiling of circulating MicroRNAs in serum of *Cysticercus pisiformis*-infected rabbits. *Genes (Basel)*. 2021;12:1591.
20. Zheng Y. High-throughput identification of miRNAs of *Taenia ovis*, a cestode threatening sheep industry. *Infect Genet Evol*. 2017;51:98-100.
21. Cucher M, Koziol U, Castillo E, et al. Expression profiling of *Echinococcus multilocularis* miRNAs throughout metacestode development in vitro. *PLoS Negl Trop Dis*. 2021;15:e0009297.
22. Guo X, Zheng Y. Expression profiling of circulating miRNAs in mouse serum in response to *Echinococcus multilocularis* infection. *Parasitology*. 2017;144:1079-1087.
23. Örsen S, Baysal İ, Yabanoglu-Ciftci S, et al. Can parasite-derived microRNAs differentiate active and inactive cystic echinococcosis patients? *Parasitol Res*. 2022;121:191-196.
24. Celik F, Tektemur A, Simsek S. miRNA based biomarkers for the early diagnosis of *Echinococcus granulosus* in experimentally infected dogs. *Vet Parasitol*. 2023;324:110075.
25. Forero DA, González-Giraldo Y, Castro-Vega LJ, Barreto GE. qPCR-based methods for expression analysis of miRNAs. *Biotechniques*. 2019;67:192-199.
26. Takei F, Akiyama M, Murata A, Sugai A, Nakatani K, Yamashita I. RT-Hpro-PCR: a MicroRNA detection system using a primer with a DNA tag. *Chembiochem*. 2020;21:477-480.
27. Usó M, Jantus-Lewintre E, Sirera R, Bremnes RM, Camps C. miRNA detection methods and clinical implications in lung cancer. *Future Oncol*. 2014;10:2279-2292.
28. Ahmad W, Gull B, Baby J, Mustafa F. A comprehensive analysis of northern versus liquid hybridization assays for mRNAs, small RNAs, and miRNAs using a non-radiolabeled approach. *Curr Issues Mol Biol*. 2021;43:457-484.
29. Jinek M, Chylinski K, Fonfara I, Hauer M, Doudna JA, Charpentier E. A programmable dual-RNA-guided DNA endonuclease in adaptive bacterial immunity. *Science*. 2012;337:816-821.
30. Chen C, Ridzon DA, Broomer AJ, et al. Real-time quantification of microRNAs by stem-loop RT-PCR. *Nucleic Acids Res*. 2005;33:e179.
31. Becker C, Hammerle-Fickinger A, Riedmaier I, Pfaffl MW. mRNA and microRNA quality control for RT-qPCR analysis. *Methods*. 2010;50:237-243.
32. Zhao B, Song J, Guan Y. Discriminative identification of miRNA let-7 family members with high specificity and sensitivity using rolling circle amplification. *Acta Biochim Biophys Sin Shanghai*. 2015;47:130-136.
33. Várallyay E, Burgyán J, Havelda Z. MicroRNA detection by northern blotting using locked nucleic acid probes. *Nat Protoc*. 2008;3:190-196.
34. Yin JQ, Zhao RC, Morris KV. Profiling microRNA expression with microarrays. *Trends Biotechnol*. 2008;26:70-76.
35. Tian W, Li P, He W, Liu C, Li Z. Rolling circle extension-actuated loop-mediated isothermal amplification (RCA-LAMP) for ultrasensitive detection of microRNAs. *Biosens Bioelectron*. 2019;128:17-22.
36. Qu XM, Ren XD, Su N, et al. Isothermal exponential amplification reactions triggered by circular templates (cEXPAR) targeting miRNA. *Mol Biol Rep*. 2023;50:3653-3659.
37. Kim TY, Kim S, Jung JH, Woo MA. Paper-based radial flow assay integrated to portable isothermal amplification chip platform for colorimetric detection of target DNA. *Biochip J*. 2023;27:1-11.
38. Chen H, Zhuang Z, Chen Y, et al. A universal platform for one-pot detection of circulating non-coding RNA combining CRISPR-Cas12a and branched rolling circle amplification. *Anal Chim Acta*. 2023;1246:340896.
39. Jin F, Xu D. A fluorescent microarray platform based on catalytic hairpin assembly for MicroRNAs detection. *Anal Chim Acta*. 2021;1173:338666.
40. Liu X, Zhao X, Yuan Y, et al. Accurate detection of lung cancer-related microRNA through CRISPR/Cas9-assisted garland rolling circle amplification. *J Thorac Dis*. 2022;14:4427-4434.
41. Wang R, Zhao X, Chen X, et al. Rolling circular amplification (RCA)-assisted CRISPR/Cas9 cleavage (RACE) for highly specific detection of multiple extracellular vesicle microRNAs. *Anal Chem*. 2020;92:2176-2185.
42. Spiliotis M, Brehm K. Axenic in vitro cultivation of *Echinococcus multilocularis* metacestode vesicles and the generation of primary cell cultures. *Methods Mol Biol*. 2009;470:245-262.
43. Ruopp MD, Perkins NJ, Whitcomb BW, Schisterman EF. Youden index and optimal cut-point estimated from observations affected by a lower limit of detection. *Biom J*. 2008;50:419-430.
44. Poon SC, Nellans K, Gorroochurn P, Chahine NO. Race, but not gender, is associated with admissions into orthopaedic residency programs. *Clin Orthop Relat Res*. 2022;480:1441-1449.
45. Ma QN, Wang M, Zheng LB, et al. RAA-Cas12a-Tg: a nucleic acid detection system for *Toxoplasma gondii* based on CRISPR-Cas12a combined with recombinase-aided amplification (RAA). *Microorganisms*. 2021;9:1644.
46. Wang Y, Zhou J, Chen Y, et al. Quantification of distinct let-7 microRNA family members by a modified stem-loop RT-qPCR. *Mol Med Rep*. 2018;17:3690-3696.
47. Krepelkova I, Mrackova T, Izakova J, et al. Evaluation of miRNA detection methods for the analytical characteristic necessary for clinical utilization. *Biotechniques*. 2019;66:277-284.
48. Tian W, Liu X, Wang G, Liu C. A hyperbranched transcription-activated CRISPR-Cas12a signal amplification strategy for sensitive microRNA sensing. *Chem Commun (Camb)*. 2020;56:13445-13448.

49. Qiu XY, Zhu LY, Zhu CS, et al. Highly effective and low-cost microRNA detection with CRISPR-Cas9. *ACS Synth Biol.* 2018;7:807-813.
50. Zhou T, Huang M, Lin J, Huang R, Xing D. High-fidelity CRISPR/Cas13a trans-cleavage-triggered rolling circle amplified DNzyme for visual profiling of microRNA. *Anal Chem.* 2021;93:2038-2044.
51. Zhou T, Huang R, Huang M, Shen J, Shan Y, Xing D. CRISPR/Cas13a powered portable electrochemiluminescence chip for ultrasensitive and specific MiRNA detection. *Adv Sci (Weinh).* 2020;7:1903661.
52. Zovoilis A, Agbemenyah HY, Agis-Balboa RC, et al. microRNA-34c is a novel target to treat dementias. *EMBO J.* 2011;30:4299-4308.
53. Yang LH, Wang SL, Tang LL, et al. Universal stem-loop primer method for screening and quantification of microRNA. *PLoS One.* 2014;9:e115293.

## SUPPORTING INFORMATION

Additional supporting information can be found online in the Supporting Information section at the end of this article.

**How to cite this article:** Wang L, Pu G, Liu T, et al. Parasite-derived microRNA let-7-5p detection for metacestodiasis based on rolling circular amplification-assisted CRISPR/Cas9. *The FASEB Journal.* 2024;38:e23708. doi:[10.1096/fj.202302449R](https://doi.org/10.1096/fj.202302449R)